

Figure 1. Summary of experimental design and data collected for this study. (A) A flow-chart summarizes the analyses that were performed. Genes are divided according to whether they show evidence for differential expression (DE) between the two parents, B73 and Mo17 and the subset of

genes that exhibit single parent expression (SPE) was then identified. The additivity of expression for all DE genes was assessed and classified. A subset of DE genes that include sequence polymorphisms and are expressed at sufficient levels were used to assess and classify cis/trans regulatory variation. (B) t-SNE visualization of all 204 samples. Log2 transformed CPM values of a set of 17,433 genes expressed (CPM  $\geq 1$ ) in at least 143 (70%) samples were used in this analysis. Principal component analysis (PCA) followed by nearest-neighbor graph-based clustering (t-SNE) was performed to display all samples in 2D space. The color indicates tissue and the shape indicates genotype. (C) The numbers of genes that are detected (Counts per Million (CPM)  $>1$  in at least two samples in each tissue) in 0-23 tissues are shown. Different colors represent the proportion out of all 23 tissues where each gene is expressed: not expressed in any tissue ("Silent"), expressed in less than 20% of tissues (Tissue specific), expressed in 20-80% tissues (Intermediate frequency) and those expressed in more than 80% tissues (Constitutive). (D) The proportion genes in each expression category (defined in panel C) that are non-syntenic (relative to other grasses including sorghum and rice) or lack any known domains (Interproscan, see methods) were compared to the background gene set (all genes).

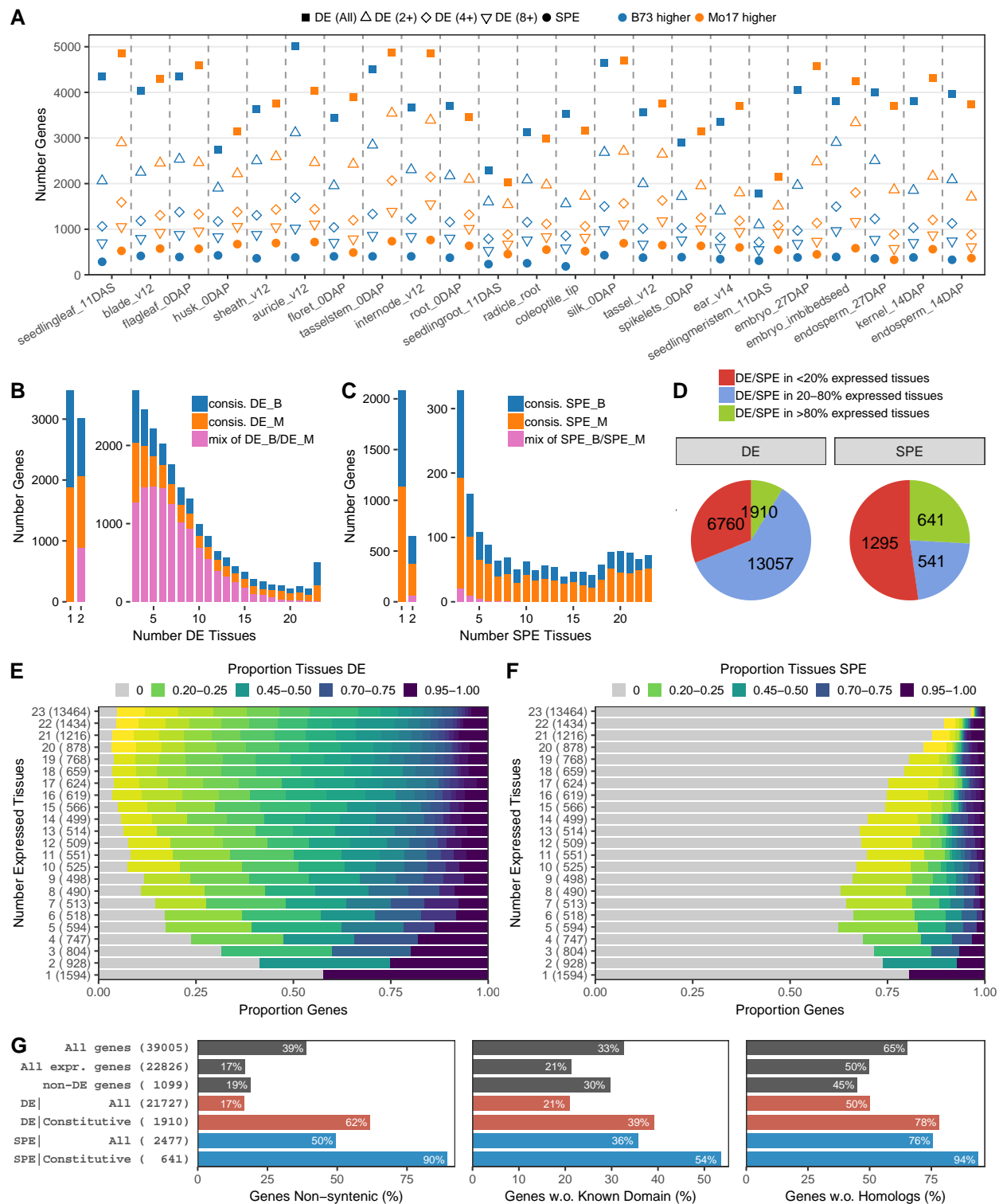


Figure 2. Analysis of developmental dynamics of differential expression. (A) The number of DE genes for each tissue is indicated by the square symbols with the genotype exhibit higher expression indicated by color (blue - B73 and orange - Mo17). Subsets of genes with >2-fold, >4-fold or >8-fold changes in expression are indicated by symbols (see legend above figure). The number of genes with single parent expression (SPE - DE genes with expression <0.1 CPM (Counts

per Million) in one parent) for each tissue is shown by the circle. (B) The number of DE genes that are detected in 1-23 tissues is shown. The color indicates which genotypes is more highly expressed as in (A) with pink indicating genes for which some tissues exhibit higher expression for B73 and other tissues with higher expressed for Mo17. (C) The numbers of SPE genes that are detected in 1-23 tissues. (D) The set of DE/SPE genes that have detectable expression in at least 10 tissues were classified according to whether the DE/SPE pattern is observed in less than 20% of expressed tissues (red, "tissue-specific), in 20-80% of expressed tissues (blue, "intermediate frequency") or more than 80% of expressed tissues (green, "constitutive"). (E-F) Characterization of DE/SPE patterns relative to presence of expression. Genes were first binned by in the number of tissues with expression (y-axis) with numbers in the parentheses indicating the sample size (corresponding to Figure 1B). Genes within each bin were further grouped by the proportion of expressed tissues showing DE/SPE patterns. Genes showing DE/SPE in none of the expressed tissues were colored in gray, while genes showing DE/SPE in at least one tissue were color coded by the proportion of tissues exhibiting DE/SPE. (G) The percentage of genes that exhibit DE or SPE patterns that are non-syntenic, lack any known domains (Interproscan) or lack any homologs in public databases was determined and compared for all genes. For the set of DE/SPE genes we also show the frequencies for the subset of genes with constitutive (DE/SPE in more than 80% expressed tissues) patterns.

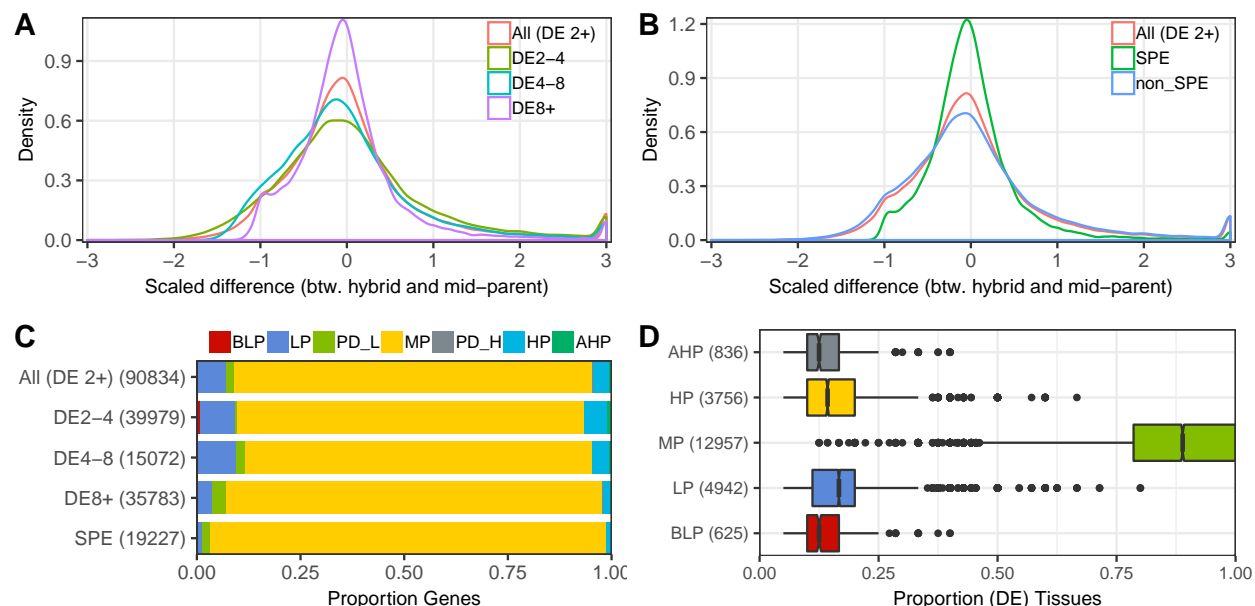


Figure 3. Classification of non-additive expression patterns. (A) The distribution of scaled difference (sometimes referred to as dominance/additivity (d/a) values) is shown. For each gene the scaled difference value is calculated as the  $(F1-MP)/(HP-MP)$  such that a value of -1 would indicate expression at the same level of the low parent, a value of 0 indicates mid-parental expression and a value of 1 indicates high parent expression levels. The d/a distributions are shown for all DE genes (DE2+), DE genes that are 2-4 fold change between parents (DE2-4), DE genes that are 4-8 fold change between parents (DE4-8), DE genes that are above 8 fold change between parents (DE8+). In (B) the scaled difference distributions are shown for all DE genes compared to SPE and non-SPE genes. (C) The proportion of genes showing different additivity patterns (BLP: below low-parent, LP: low-parent, MP: mid-parent, HP: high-parent and AHP: above high-parent) was determined for aforementioned gene sets. The numbers in parentheses are total number of DE instances (passing given thresholds) summed across 20 non-seed tissues. (D) The set of genes that are DE in at least five tissues were used to examine the prevalence of additivity patterns across development with the number of genes in each set indicated in parentheses. For each gene we determined the proportion of tissues exhibiting the additivity pattern of interest and use a box-plot to visualize the distribution of values.

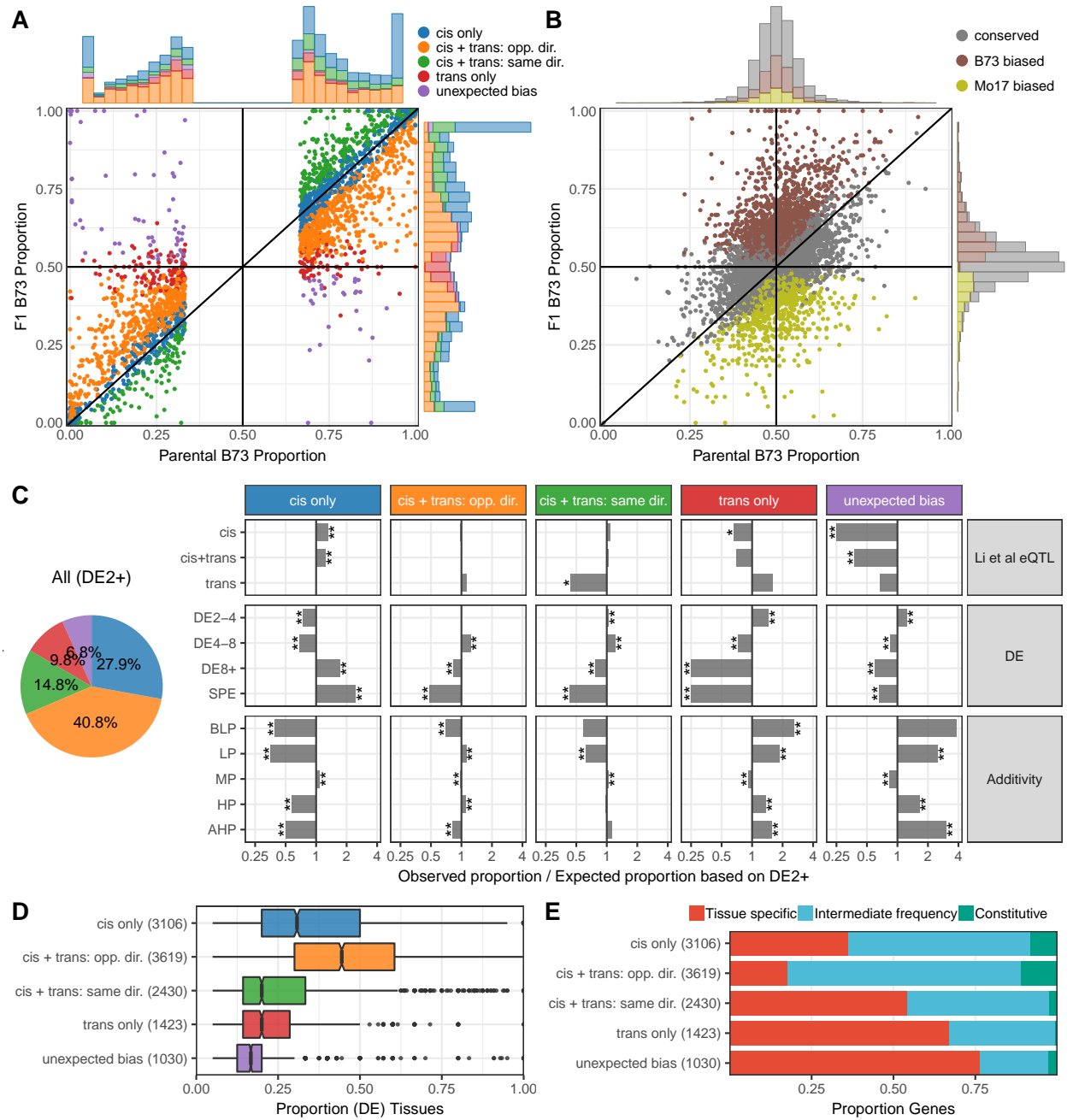


Figure 4. Analysis of biased allelic expression patterns and regulatory variation classification across tissues. (A-B) A scatterplot shows the parental B73 allele ratio (x-axis,  $CPM_B/(CPM_B + CPM_M)$ ) and hybrid B73 allele ratio (y-axis) for DE genes (A) and non-DE genes (B) in maize root tissue. The colors represent different regulatory variation classifications determined for each gene (see methods). (C) The pie-chart (left) shows the proportion of all differentially expressed genes (between the two parents) that were assigned to different regulatory mechanisms across all 20 non-endosperm tissues. The plots on the right show the enrichment or depletion (as fold change relative to background proportion from the left pie-chart) for subsets of genes for each regulatory variation classification. The subsets of genes include different levels of fold change in expression (DE2-4, DE4-8, DE8+ and SPE), different additivity patterns (BLP, LP, MP, HP, AHP) and genes that were characterized by previous eQTL study (in Shoot Apex Meristem Li et al.,

2013) to be regulated by only cis-eQTL(s), only trans-eQTL(s) or by both cis-eQTL(s) and trans-eQTL(s). For each subset of genes the proportion of each regulatory classification was compared to background proportion (left pie-chart) with the ratio plotted as bars along x-axis. P-values were determined using hypergeometric test (lower.tail = FALSE for enrichment and lower.tail = TRUE for depletion) and labelled as "\*" (P < 0.01) or "\*\*\*" (P < 0.001). (D-E) For genes that are DE and have allele-specific expression data in at least five tissues we assessed the consistency of regulation variation classifications. In (D) the subset of genes that are classified into each pattern in at least one tissue were used to assess the proportion of tissues that show this pattern. In (E) all genes classified into a specific pattern in at least one tissue were used to assess whether that classification was tissue specific (showing that pattern in less than 20% of DE tissues), intermediate frequency (20%-80% DE tissues) or constitutive (more than 80% of DE tissues).

Table S1. Samples used in this study.

Sample	Tissue	Genotype	Rep	Condition	TotalPairs	TrimmedPairs	MappingRate	UniqueMappingRate
BR001	blade_v12	B73	1	Field	9,456,463	9,367,415	98.4%	91.6%
BR002	blade_v12	B73	2	Field	10,614,657	10,530,486	98.5%	92.9%
BR003	blade_v12	Mo17	1	Field	9,456,508	9,374,216	92.2%	87.1%
BR004	blade_v12	B73	3	Field	10,983,851	10,894,598	98.4%	92.0%
BR005	blade_v12	Mo17	2	Field	9,878,003	9,791,778	92.5%	86.6%
BR006	blade_v12	BxM	1	Field	13,109,236	13,005,210	95.2%	83.8%
BR007	blade_v12	Mo17	3	Field	10,136,440	10,049,207	94.2%	41.5%
BR008	blade_v12	BxM	2	Field	9,958,057	9,762,863	91.8%	81.6%
BR009	blade_v12	BxM	3	Field	10,368,573	10,283,237	95.1%	88.1%
BR010	auricle_v12	B73	1	Field	12,161,908	12,062,687	97.4%	92.3%
BR011	auricle_v12	B73	2	Field	8,756,804	8,681,487	97.7%	91.8%
BR012	auricle_v12	B73	3	Field	9,205,753	9,115,520	98.4%	93.5%
BR013	auricle_v12	Mo17	1	Field	12,629,990	12,534,713	92.4%	68.5%
BR014	auricle_v12	Mo17	2	Field	12,106,840	12,015,331	91.9%	85.6%
BR015	auricle_v12	Mo17	3	Field	12,789,833	12,688,046	91.9%	86.2%
BR016	auricle_v12	BxM	1	Field	13,001,085	12,894,656	95.2%	90.2%
BR017	auricle_v12	BxM	2	Field	10,302,708	10,221,028	95.0%	89.9%
BR018	auricle_v12	BxM	3	Field	10,717,426	10,612,110	93.9%	88.7%
BR019	sheath_v12	B73	1	Field	11,363,325	11,252,448	98.3%	92.6%
BR020	sheath_v12	B73	2	Field	11,653,190	11,560,292	98.5%	92.6%
BR021	sheath_v12	B73	3	Field	10,397,926	10,313,536	98.3%	91.6%
BR022	sheath_v12	Mo17	1	Field	10,300,996	10,223,999	91.0%	84.9%
BR023	sheath_v12	Mo17	2	Field	10,610,559	10,504,881	90.6%	84.5%
BR024	sheath_v12	Mo17	3	Field	10,818,591	10,732,498	91.1%	85.2%
BR025	sheath_v12	BxM	1	Field	10,460,515	10,317,769	89.3%	80.0%
BR026	sheath_v12	BxM	2	Field	13,454,079	13,205,917	90.2%	84.6%
BR027	sheath_v12	BxM	3	Field	10,947,765	10,796,345	93.0%	85.9%
BR028	internode_v12	B73	1	Field	11,704,246	11,566,394	97.2%	92.1%
BR032	internode_v12	Mo17	1	Field	18,897,584	18,677,705	90.6%	84.7%
BR030	internode_v12	B73	2	Field	11,511,692	11,382,708	98.1%	91.9%
BR031	internode_v12	Mo17	2	Field	11,675,275	11,554,947	90.9%	85.9%
BR029	internode_v12	B73	3	Field	7,280,863	7,207,320	97.4%	90.0%
BR033	internode_v12	Mo17	3	Field	11,763,511	11,618,868	90.2%	85.3%
BR034	internode_v12	BxM	1	Field	11,446,013	11,309,805	94.4%	89.6%
BR035	internode_v12	BxM	2	Field	10,813,338	10,680,875	94.0%	88.2%
BR036	internode_v12	BxM	3	Field	12,185,937	12,056,501	94.8%	89.3%
BR037	tassel_v12	B73	1	Field	11,869,598	11,767,998	98.2%	87.0%
BR038	tassel_v12	B73	2	Field	13,057,367	12,963,185	98.2%	80.5%
BR039	tassel_v12	B73	3	Field	11,971,434	11,876,376	98.4%	86.7%
BR040	tassel_v12	Mo17	1	Field	10,198,649	10,119,317	92.8%	78.9%
BR041	tassel_v12	Mo17	2	Field	9,541,534	9,458,818	92.5%	86.3%
BR042	tassel_v12	Mo17	3	Field	12,122,651	12,028,360	92.8%	73.7%
BR043	tassel_v12	BxM	1	Field	11,577,660	11,490,867	94.8%	87.3%
BR044	tassel_v12	BxM	2	Field	9,209,055	9,080,007	94.3%	81.8%
BR045	tassel_v12	BxM	3	Field	11,345,207	11,254,362	94.8%	87.8%
BR046	ear_v14	B73	1	Field	10,279,754	10,201,193	97.1%	77.0%
BR047	ear_v14	B73	2	Field	10,892,889	10,799,410	98.2%	88.4%
BR048	ear_v14	B73	3	Field	10,423,251	10,340,695	98.2%	87.5%
BR049	ear_v14	Mo17	1	Field	11,158,750	11,087,463	93.4%	88.3%
BR050	ear_v14	Mo17	2	Field	10,615,140	10,544,171	92.6%	87.5%
BR051	ear_v14	Mo17	3	Field	10,130,338	10,058,913	93.5%	88.5%
BR052	ear_v14	BxM	1	Field	9,779,316	9,705,723	96.0%	90.8%
BR053	ear_v14	BxM	2	Field	10,765,471	10,691,005	96.1%	90.7%
BR054	ear_v14	BxM	3	Field	10,866,113	10,786,414	96.0%	90.8%
BR055	silk_ODAP	B73	1	Field	10,460,214	10,354,824	98.3%	92.9%
BR056	silk_ODAP	B73	2	Field	10,094,098	10,015,873	98.3%	87.9%
BR057	silk_ODAP	B73	3	Field	9,351,362	9,259,488	98.2%	92.8%



Table S1. Samples used in this study. (continued)

Sample	Tissue	Genotype	Rep	Condition	TotalPairs	TrimmedPairs	MappingRate	UniqueMappingRate
BR058	silk_ODAP	Mo17	1	Field	9,154,814	9,077,113	91.2%	84.3%
BR059	silk_ODAP	Mo17	2	Field	9,271,623	9,184,908	91.2%	85.6%
BR060	silk_ODAP	Mo17	3	Field	8,610,999	8,539,340	91.1%	86.0%
BR061	silk_ODAP	BxM	1	Field	12,378,233	12,274,018	94.4%	88.3%
BR062	silk_ODAP	BxM	2	Field	11,117,019	10,918,321	93.2%	87.6%
BR063	silk_ODAP	BxM	3	Field	12,831,768	12,714,257	95.0%	89.4%
BR064	spikelets_ODAP	B73	1	Field	12,862,409	12,756,383	97.9%	92.1%
BR065	spikelets_ODAP	B73	2	Field	13,140,565	13,016,984	98.5%	92.8%
BR066	spikelets_ODAP	B73	3	Field	12,366,130	12,261,404	98.5%	92.9%
BR067	spikelets_ODAP	Mo17	1	Field	12,302,995	12,214,346	92.0%	85.9%
BR068	spikelets_ODAP	Mo17	2	Field	12,364,997	12,266,006	92.3%	85.0%
BR069	spikelets_ODAP	Mo17	3	Field	12,363,396	12,261,701	92.5%	86.7%
BR070	spikelets_ODAP	BxM	1	Field	10,329,056	10,246,209	95.4%	89.4%
BR071	spikelets_ODAP	BxM	2	Field	12,278,485	12,184,457	95.4%	89.8%
BR072	spikelets_ODAP	BxM	3	Field	12,426,693	12,323,355	95.7%	89.9%
BR073	husk_ODAP	B73	1	Field	12,468,897	12,338,745	98.3%	92.5%
BR074	husk_ODAP	B73	2	Field	11,486,069	11,389,989	98.3%	92.2%
BR075	husk_ODAP	B73	3	Field	11,705,643	11,598,042	98.3%	92.1%
BR076	husk_ODAP	Mo17	1	Field	12,818,182	12,713,872	92.1%	83.4%
BR077	husk_ODAP	Mo17	2	Field	12,761,502	12,635,684	91.4%	85.5%
BR078	husk_ODAP	Mo17	3	Field	12,826,901	12,717,414	91.9%	85.6%
BR079	husk_ODAP	BxM	1	Field	12,503,981	12,395,438	94.7%	89.1%
BR080	husk_ODAP	BxM	2	Field	11,607,643	11,406,667	93.7%	88.0%
BR081	husk_ODAP	BxM	3	Field	13,790,861	13,666,823	95.3%	89.8%
BR082	tasselstem_ODAP	B73	1	Field	12,451,564	12,349,251	97.8%	92.1%
BR083	tasselstem_ODAP	B73	2	Field	12,221,050	12,112,847	98.3%	92.7%
BR084	tasselstem_ODAP	B73	3	Field	11,567,848	11,471,842	98.0%	88.0%
BR085	tasselstem_ODAP	Mo17	1	Field	9,540,165	9,463,815	90.5%	83.1%
BR086	tasselstem_ODAP	Mo17	2	Field	9,089,631	9,011,444	91.1%	85.8%
BR087	tasselstem_ODAP	Mo17	3	Field	9,244,929	9,157,904	91.2%	85.7%
BR088	tasselstem_ODAP	BxM	1	Field	8,876,713	8,797,378	94.5%	88.0%
BR089	tasselstem_ODAP	BxM	2	Field	9,021,520	8,943,627	93.9%	88.0%
BR090	tasselstem_ODAP	BxM	3	Field	9,072,250	8,993,652	94.2%	87.0%
BR091	floret_ODAP	B73	1	Field	10,046,688	9,917,126	98.1%	89.5%
BR092	floret_ODAP	B73	2	Field	10,344,979	10,247,053	98.3%	88.6%
BR093	floret_ODAP	B73	3	Field	9,586,452	9,469,113	98.1%	89.7%
BR094	floret_ODAP	Mo17	1	Field	9,591,540	9,496,979	90.9%	83.0%
BR095	floret_ODAP	Mo17	2	Field	10,171,616	10,050,093	90.1%	83.2%
BR096	floret_ODAP	Mo17	3	Field	8,968,665	8,870,021	91.6%	84.9%
BR097	floret_ODAP	BxM	1	Field	8,971,648	8,871,487	95.1%	89.1%
BR098	floret_ODAP	BxM	2	Field	9,125,085	8,871,603	93.3%	86.3%
BR099	floret_ODAP	BxM	3	Field	10,114,073	10,000,848	95.0%	86.9%
BR118	kernel_14DAP	B73	1	Field	10,936,328	10,843,315	98.3%	87.3%
BR119	kernel_14DAP	B73	2	Field	11,056,044	10,956,542	98.4%	89.0%
BR120	kernel_14DAP	B73	3	Field	10,542,981	10,452,024	98.3%	86.7%
BR121	kernel_14DAP	Mo17	1	Field	13,288,857	13,186,732	94.6%	85.2%
BR122	kernel_14DAP	Mo17	2	Field	13,244,937	13,134,240	94.5%	86.1%
BR123	kernel_14DAP	Mo17	3	Field	11,612,393	11,504,790	94.3%	83.0%
BR124	kernel_14DAP	BxM	1	Field	12,287,598	12,188,660	97.5%	82.4%
BR125	kernel_14DAP	BxM	2	Field	11,390,752	11,303,494	97.4%	82.3%
BR126	kernel_14DAP	BxM	3	Field	10,802,003	10,718,433	97.5%	82.8%
BR100	flagleaf_ODAP	B73	1	Field	8,870,907	8,779,729	98.3%	90.6%
BR101	flagleaf_ODAP	B73	2	Field	8,927,886	8,852,968	98.5%	92.2%
BR102	flagleaf_ODAP	B73	3	Field	9,310,919	9,227,730	98.6%	92.3%
BR103	flagleaf_ODAP	Mo17	1	Field	12,454,393	12,351,934	92.0%	87.2%
BR104	flagleaf_ODAP	Mo17	2	Field	11,124,928	11,016,585	92.4%	86.5%
BR105	flagleaf_ODAP	Mo17	3	Field	9,139,066	9,063,499	92.0%	86.9%

Table S1. Samples used in this study. (continued)

Sample	Tissue	Genotype	Rep	Condition	TotalPairs	TrimmedPairs	MappingRate	UniqueMappingRate
BR106	flagleaf_0DAP	BxM	1	Field	8,237,380	8,161,554	95.1%	89.4%
BR107	flagleaf_0DAP	BxM	2	Field	11,375,396	11,265,249	95.3%	89.9%
BR108	flagleaf_0DAP	BxM	3	Field	8,739,031	8,651,672	95.2%	89.0%
BR109	root_0DAP	B73	1	Field	12,780,458	12,681,574	98.7%	94.0%
BR110	root_0DAP	B73	2	Field	11,071,413	10,726,484	95.8%	91.2%
BR111	root_0DAP	B73	3	Field	14,352,722	14,232,937	98.7%	94.2%
BR112	root_0DAP	Mo17	1	Field	13,432,400	13,337,049	91.9%	87.2%
BR113	root_0DAP	Mo17	2	Field	11,241,291	11,148,033	91.9%	87.7%
BR114	root_0DAP	Mo17	3	Field	11,748,397	11,657,233	91.8%	87.4%
BR115	root_0DAP	BxM	1	Field	12,447,495	12,322,988	94.7%	90.3%
BR116	root_0DAP	BxM	2	Field	13,501,613	13,391,660	95.0%	90.7%
BR117	root_0DAP	BxM	3	Field	12,014,758	11,917,490	95.3%	90.9%
BR130	endosperm_14DAP	B73	1	Field	7,971,614	7,908,501	98.4%	87.7%
BR131	endosperm_14DAP	B73	2	Field	8,354,751	8,297,059	98.6%	87.4%
BR132	endosperm_14DAP	B73	3	Field	8,106,969	8,043,877	98.4%	87.1%
BR133	endosperm_14DAP	Mo17	1	Field	7,996,705	7,944,390	95.1%	86.0%
BR134	endosperm_14DAP	Mo17	2	Field	7,111,069	7,056,236	95.0%	86.1%
BR135	endosperm_14DAP	Mo17	3	Field	7,053,101	7,003,061	94.9%	85.4%
BR136	endosperm_14DAP	BxM	1	Field	7,342,993	7,293,685	97.3%	80.3%
BR137	endosperm_14DAP	BxM	2	Field	7,408,587	7,282,363	95.5%	82.6%
BR138	endosperm_14DAP	BxM	3	Field	8,295,102	8,242,013	97.5%	81.5%
BR142	embryo_27DAP	B73	1	Field	7,372,483	7,316,640	98.5%	86.8%
BR143	embryo_27DAP	B73	2	Field	7,042,198	6,983,724	98.7%	90.0%
BR144	embryo_27DAP	B73	3	Field	6,553,609	6,498,382	98.3%	87.1%
BR145	embryo_27DAP	Mo17	1	Field	7,077,358	7,002,686	91.6%	83.7%
BR146	embryo_27DAP	Mo17	2	Field	7,533,408	7,451,111	91.3%	83.5%
BR147	embryo_27DAP	Mo17	3	Field	8,261,322	8,162,520	92.3%	47.1%
BR148	embryo_27DAP	BxM	1	Field	7,602,835	7,530,655	94.5%	84.1%
BR149	embryo_27DAP	BxM	2	Field	8,456,705	8,336,995	94.2%	85.4%
BR150	embryo_27DAP	BxM	3	Field	8,081,181	7,993,598	94.9%	83.0%
BR154	endosperm_27DAP	B73	1	Field	17,736,115	17,600,317	98.3%	68.2%
BR155	endosperm_27DAP	B73	2	Field	17,169,716	17,057,377	98.3%	68.4%
BR156	endosperm_27DAP	B73	3	Field	18,730,409	18,611,675	98.4%	69.2%
BR157	endosperm_27DAP	Mo17	1	Field	14,649,158	14,549,188	96.2%	66.5%
BR158	endosperm_27DAP	Mo17	2	Field	15,811,476	15,702,263	96.4%	66.1%
BR159	endosperm_27DAP	Mo17	3	Field	13,053,684	12,967,048	96.6%	67.5%
BR160	endosperm_27DAP	BxM	1	Field	14,814,247	14,719,774	97.8%	71.6%
BR161	endosperm_27DAP	BxM	2	Field	14,413,309	14,133,430	95.7%	67.7%
BR162	endosperm_27DAP	BxM	3	Field	14,883,939	14,783,781	97.7%	68.9%
BR166	coleoptile_tip	B73	1	Growth chamber	12,267,403	12,126,234	98.0%	89.7%
BR167	coleoptile_tip	B73	2	Growth chamber	11,485,549	11,384,771	98.4%	93.3%
BR168	coleoptile_tip	B73	3	Growth chamber	12,399,486	12,290,630	98.5%	91.7%
BR169	coleoptile_tip	Mo17	1	Growth chamber	11,947,303	11,849,179	92.4%	87.4%
BR170	coleoptile_tip	Mo17	2	Growth chamber	12,242,354	12,126,048	92.5%	87.4%
BR171	coleoptile_tip	Mo17	3	Growth chamber	13,259,951	13,138,932	92.4%	86.6%
BR172	coleoptile_tip	BxM	1	Growth chamber	12,391,702	12,284,694	95.3%	90.0%
BR173	coleoptile_tip	BxM	2	Growth chamber	12,048,829	11,802,713	94.0%	88.8%
BR174	coleoptile_tip	BxM	3	Growth chamber	12,187,226	12,068,545	95.1%	73.1%
BR175	radicle_root	B73	1	Growth chamber	12,295,498	12,171,020	97.0%	92.8%
BR176	radicle_root	B73	2	Growth chamber	11,534,982	11,416,060	98.1%	93.0%
BR177	radicle_root	B73	3	Growth chamber	10,646,209	10,526,034	97.8%	92.8%
BR178	radicle_root	Mo17	1	Growth chamber	12,066,875	11,965,649	90.8%	84.2%
BR179	radicle_root	Mo17	2	Growth chamber	11,661,817	11,558,386	90.2%	85.7%
BR180	radicle_root	Mo17	3	Growth chamber	10,959,894	10,841,662	90.1%	85.5%
BR181	radicle_root	BxM	1	Growth chamber	13,122,821	13,004,621	94.2%	89.9%
BR182	radicle_root	BxM	2	Growth chamber	12,468,832	12,358,623	94.8%	90.2%
BR183	radicle_root	BxM	3	Growth chamber	11,587,217	11,485,773	94.1%	89.5%

Table S1. Samples used in this study. (continued)

Sample	Tissue	Genotype	Rep	Condition	TotalPairs	TrimmedPairs	MappingRate	UniqueMappingRate
BR184	embryo_imbibedseed	B73	1	Growth chamber	16,521,544	16,009,522	98.4%	86.6%
BR242	embryo_imbibedseed	B73	2	Growth chamber	18,100,445	17,634,613	98.4%	87.7%
BR243	embryo_imbibedseed	B73	3	Growth chamber	16,539,617	16,051,406	98.4%	88.7%
BR245	embryo_imbibedseed	Mo17	1	Growth chamber	15,060,983	14,635,237	91.8%	78.2%
BR188	embryo_imbibedseed	Mo17	2	Growth chamber	19,136,137	18,583,167	91.9%	77.8%
BR227	embryo_imbibedseed	Mo17	3	Growth chamber	10,606,785	10,249,652	92.2%	62.6%
BR191	embryo_imbibedseed	BxM	1	Growth chamber	12,528,211	11,753,391	95.2%	83.8%
BR192	embryo_imbibedseed	BxM	2	Growth chamber	16,939,295	16,506,855	95.8%	84.8%
BR193	seedlingleaf_11DAS	B73	1	Growth chamber	12,931,365	12,562,955	98.4%	90.7%
BR194	seedlingleaf_11DAS	B73	2	Growth chamber	12,993,398	12,476,399	98.7%	91.5%
BR195	seedlingleaf_11DAS	B73	3	Growth chamber	12,944,343	12,533,704	98.7%	91.8%
BR196	seedlingleaf_11DAS	Mo17	1	Growth chamber	13,154,046	12,759,277	91.3%	83.2%
BR197	seedlingleaf_11DAS	Mo17	2	Growth chamber	14,456,660	14,047,653	91.8%	85.8%
BR198	seedlingleaf_11DAS	Mo17	3	Growth chamber	12,627,543	12,111,783	91.5%	82.8%
BR199	seedlingleaf_11DAS	BxM	1	Growth chamber	13,369,929	12,922,403	95.2%	87.0%
BR200	seedlingleaf_11DAS	BxM	2	Growth chamber	12,269,095	11,890,258	94.9%	88.5%
BR201	seedlingleaf_11DAS	BxM	3	Growth chamber	16,931,135	16,451,260	95.4%	86.3%
BR202	seedlingroot_11DAS	B73	1	Growth chamber	14,286,923	13,837,005	98.3%	92.4%
BR203	seedlingroot_11DAS	B73	2	Growth chamber	13,799,806	13,493,069	98.5%	93.1%
BR204	seedlingroot_11DAS	B73	3	Growth chamber	12,973,928	12,661,827	98.6%	93.2%
BR187	embryo_imbibedseed	Mo17	4	Growth chamber	12,018,006	11,651,375	90.8%	74.2%
BR206	seedlingroot_11DAS	Mo17	1	Growth chamber	11,969,669	11,569,090	90.5%	84.8%
BR208	seedlingroot_11DAS	BxM	1	Growth chamber	14,247,885	13,919,656	95.2%	88.8%
BR209	seedlingroot_11DAS	BxM	2	Growth chamber	12,311,137	11,773,916	95.0%	89.2%
BR211	seedlingmeristem_11DAS	B73	1	Growth chamber	15,300,678	14,943,561	98.7%	93.6%
BR212	seedlingmeristem_11DAS	B73	2	Growth chamber	13,228,641	12,892,735	98.9%	93.1%
BR213	seedlingmeristem_11DAS	B73	3	Growth chamber	14,690,786	14,301,943	98.9%	93.1%
BR214	seedlingmeristem_11DAS	Mo17	1	Growth chamber	17,091,762	16,707,591	93.7%	88.4%
BR215	seedlingmeristem_11DAS	Mo17	2	Growth chamber	14,961,784	14,610,501	93.7%	88.6%
BR216	seedlingmeristem_11DAS	Mo17	3	Growth chamber	14,085,672	13,755,241	93.9%	88.9%
BR217	seedlingmeristem_11DAS	BxM	1	Growth chamber	15,456,137	15,088,536	96.4%	91.4%
BR218	seedlingmeristem_11DAS	BxM	2	Growth chamber	14,791,193	14,459,872	96.5%	89.3%
BR219	seedlingmeristem_11DAS	BxM	3	Growth chamber	13,255,400	12,905,133	96.4%	91.0%

Table S2. Enriched Gene Ontology (GO) terms for identified gene sets.

Gene set	GO	P-value	GO name
<b>All genes</b>			
Constitutive	GO:0005739	3.08e-22	mitochondrion
	GO:0022625	1.45e-11	cytosolic large ribosomal subunit
	GO:0006412	4.17e-11	translation
	GO:0005774	7.24e-10	vacuolar membrane
	GO:0009793	2.54e-09	embryo development ending in seed dormancy
	GO:0000398	3.25e-06	mRNA splicing, via spliceosome
Silent	GO:0005743	4.24e-05	mitochondrial inner membrane
	GO:0005654	4.47e-09	nucleoplasm
	GO:0043161	3.49e-06	proteasome-mediated ubiquitin-dependent protein catabolic process
	GO:0005737	2.47e-05	cytoplasm
<b>non-DEGs btw. B73 and Mo17</b>			
Above-Parent	GO:0022625	1.36e-08	cytosolic large ribosomal subunit
	GO:0042256	1.43e-05	mature ribosome assembly
	GO:0002181	4.30e-05	cytoplasmic translation
	GO:0009941	1.85e-04	chloroplast envelope
	GO:0010287	2.02e-04	plastoglobule
	GO:0009535	1.93e-03	chloroplast thylakoid membrane
	GO:0005774	2.09e-03	vacuolar membrane
	GO:0006412	4.39e-03	translation
Below-Parent	GO:0022625	1.09e-22	cytosolic large ribosomal subunit
	GO:0042256	2.63e-20	mature ribosome assembly
	GO:0002181	4.38e-13	cytoplasmic translation
	GO:0022627	5.96e-13	cytosolic small ribosomal subunit
	GO:0006412	6.76e-13	translation
	GO:0048046	4.04e-12	apoplast
	GO:0005794	9.05e-12	Golgi apparatus
	GO:0042788	8.01e-09	polysomal ribosome
	GO:0005774	4.04e-08	vacuolar membrane
	GO:0005618	1.88e-06	cell wall
	GO:0009506	3.10e-05	plasmodesma
	GO:0046686	7.22e-05	response to cadmium ion
	GO:0000028	4.78e-04	ribosomal small subunit assembly
	GO:0009735	1.23e-03	response to cytokinin
	GO:0005886	1.23e-03	plasma membrane
	GO:0009409	2.49e-03	response to cold
	GO:0009651	3.26e-03	response to salt stress
<b>DEGs btw. B73 and Mo17</b>			
HP/AHP	GO:0009535	7.76e-31	chloroplast thylakoid membrane
	GO:0009941	9.82e-19	chloroplast envelope
	GO:0009570	3.78e-16	chloroplast stroma
	GO:0009768	6.89e-08	photosynthesis, light harvesting in photosystem I
	GO:0009507	2.61e-06	chloroplast
	GO:0009773	3.32e-06	photosynthetic electron transport in photosystem I
	GO:0010287	6.58e-06	plastoglobule
	GO:0031977	1.49e-05	thylakoid lumen
	GO:0016036	2.32e-05	cellular response to phosphate starvation
	GO:0010027	9.02e-05	thylakoid membrane organization
LP/BLP	GO:0005886	6.65e-08	plasma membrane

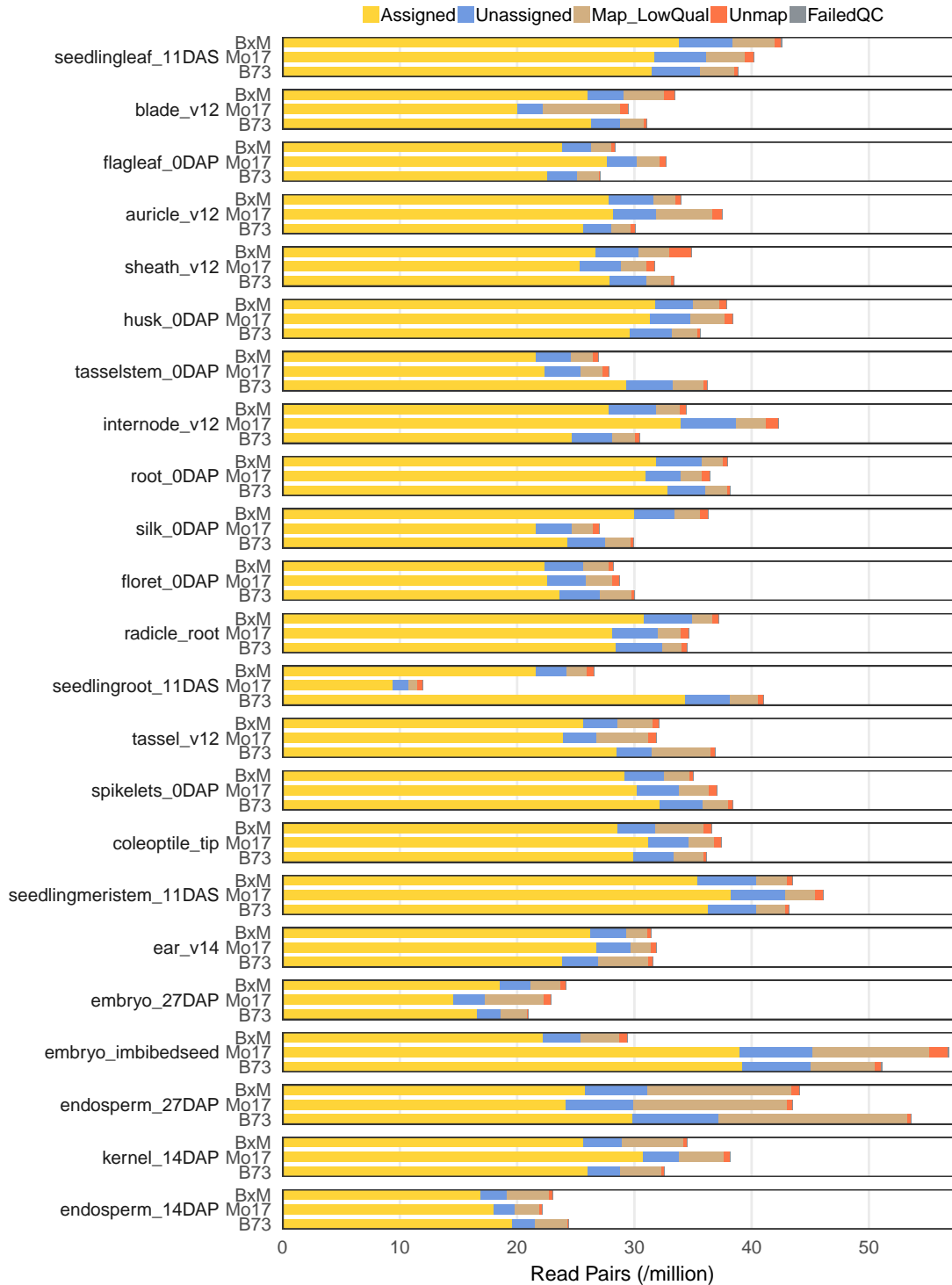


Figure S1. Summary of read mapping statistics. For each tissue / genotype combination we show the number of read pairs (in millions) mapped to the maize B73 AGPv4 reference, and the proportion of reads that failed QC (failedQC), failed to map to the genome (Unmap), mapped in multiple locations (Map\_LowQual), mapped in high quality to intergenic regions (Unassigned) as well as high quality reads assigned to genes (Assigned).

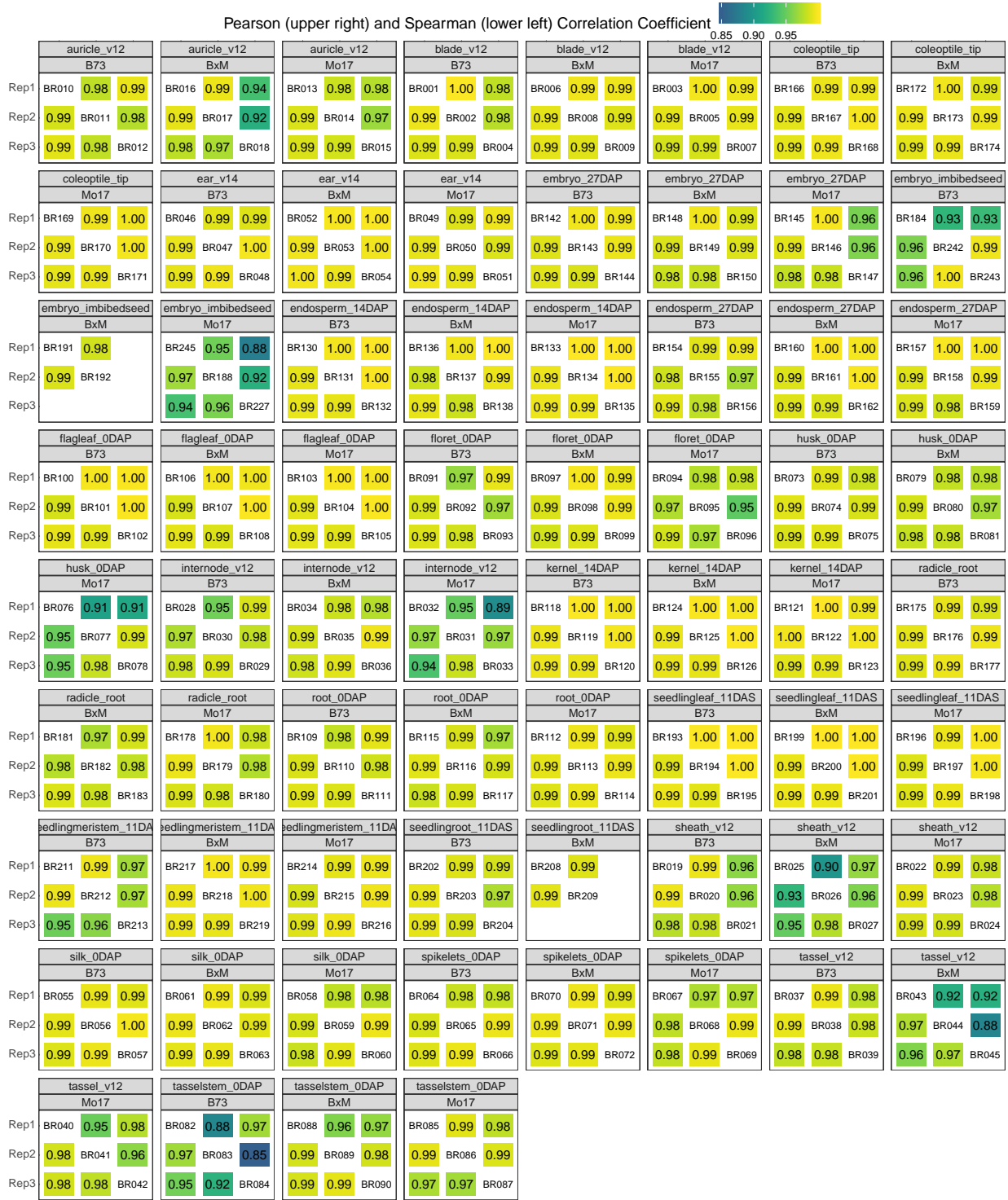


Figure S2. Consistency between biology replicates of each sample. Each panel shows a heatmap of the correlations between biological replicates for each tissue-genotype combination. These show both the Pearson (upper right half) and Spearman (lower left half) correlation values of gene expression levels (FPKMs) between each pair of replicates. The subset of 14,216 genes with CPM >1 in at least 90% samples were used in this analysis.

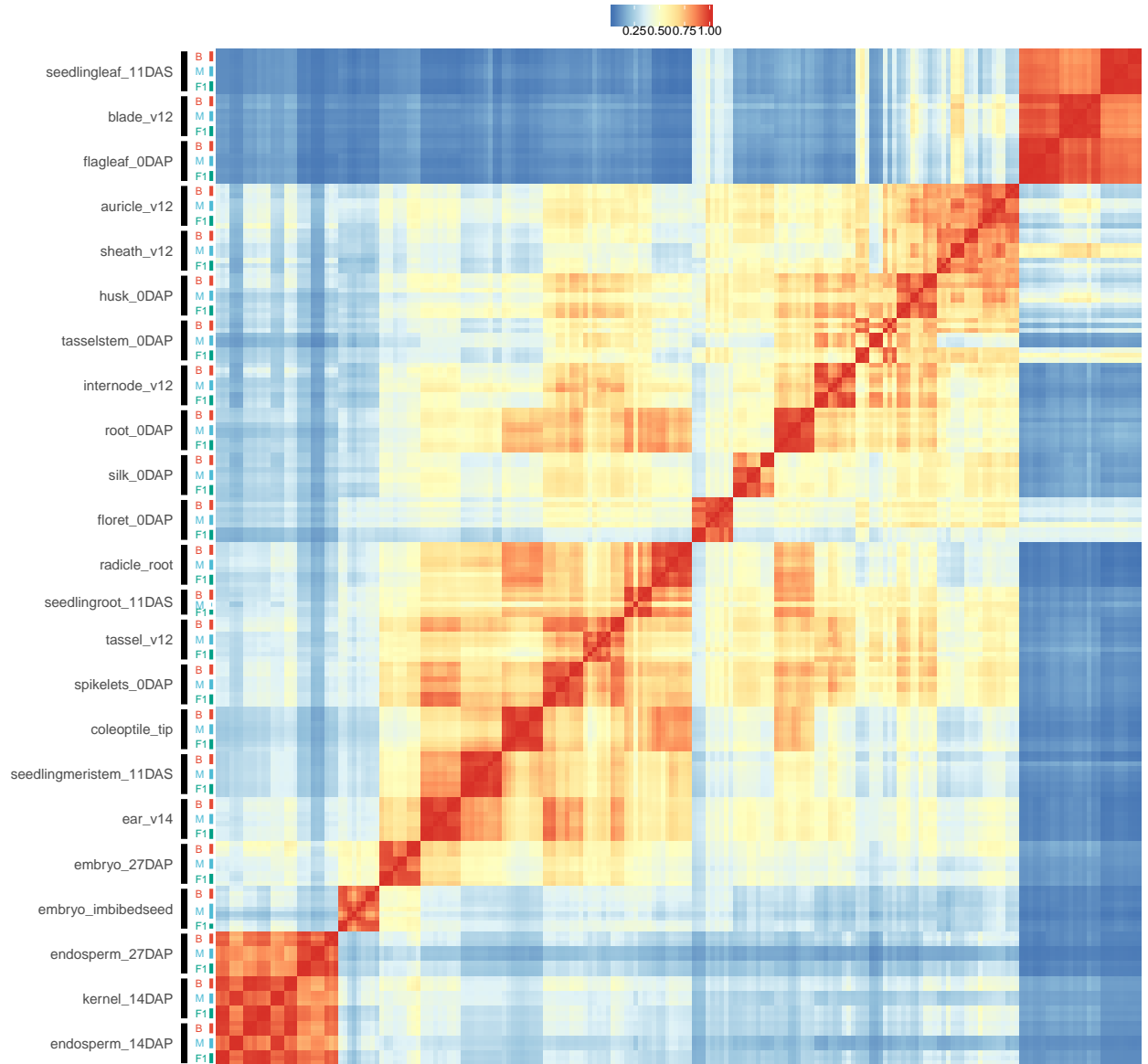


Figure S3. Distance matrix heatmap between all samples. Pearson correlation coefficients based on gene expression levels (FPKMs) between each pair of samples were shown as a heatmap. The subset of 14,216 genes with CPM >1 in at least 90% samples were used in this analysis.

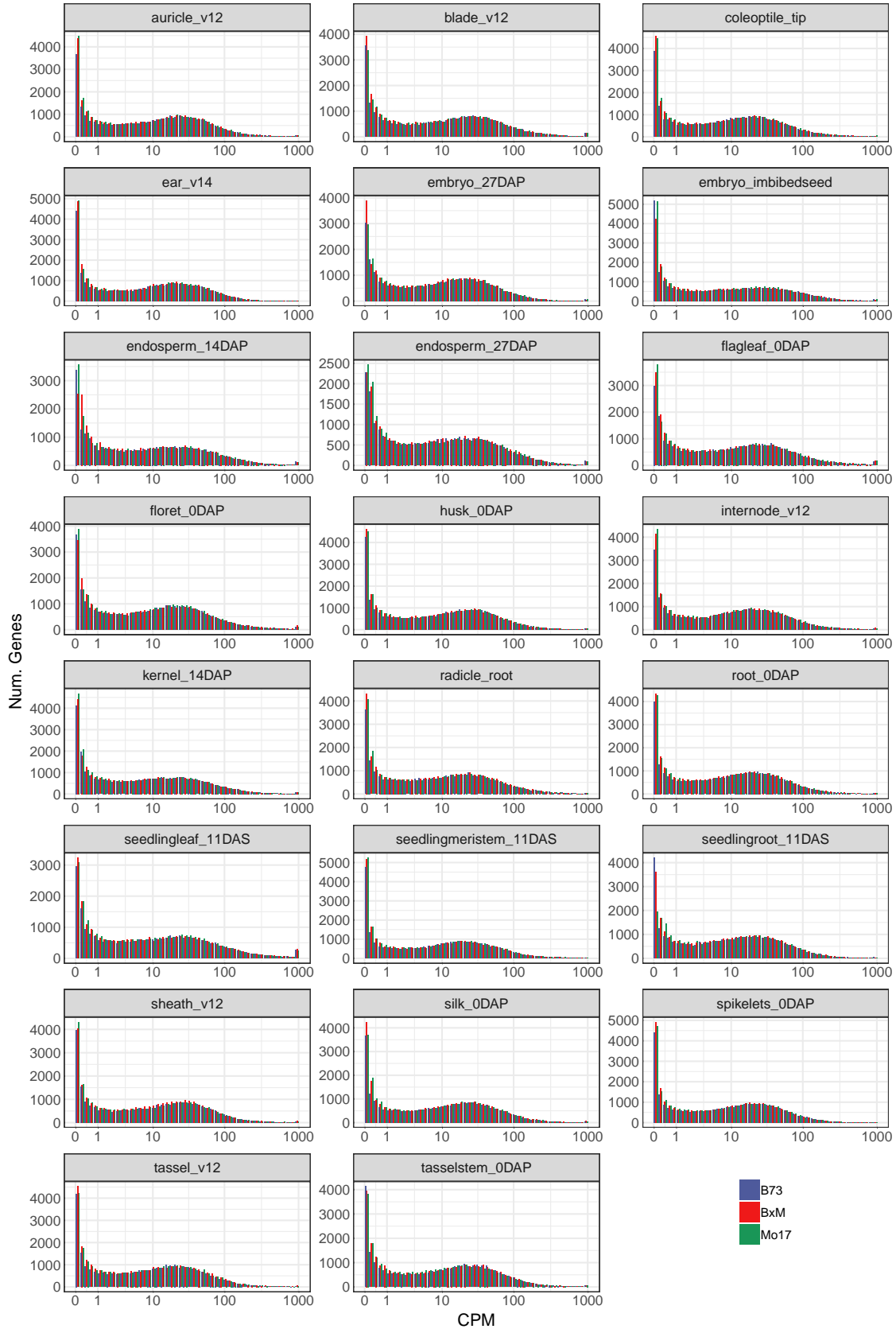


Figure S4. The distribution of gene CPM (Counts per Million) values is shown for B73, Mo17



and hybrid in each tissue. The expression values are normalized using the TMM normalization approach implemented in the edgeR (see methods). Genes with no reads (CPM=0) are not shown. The first bar in each plot shows genes with CPM that is  $>0$  and  $<0.2$ .

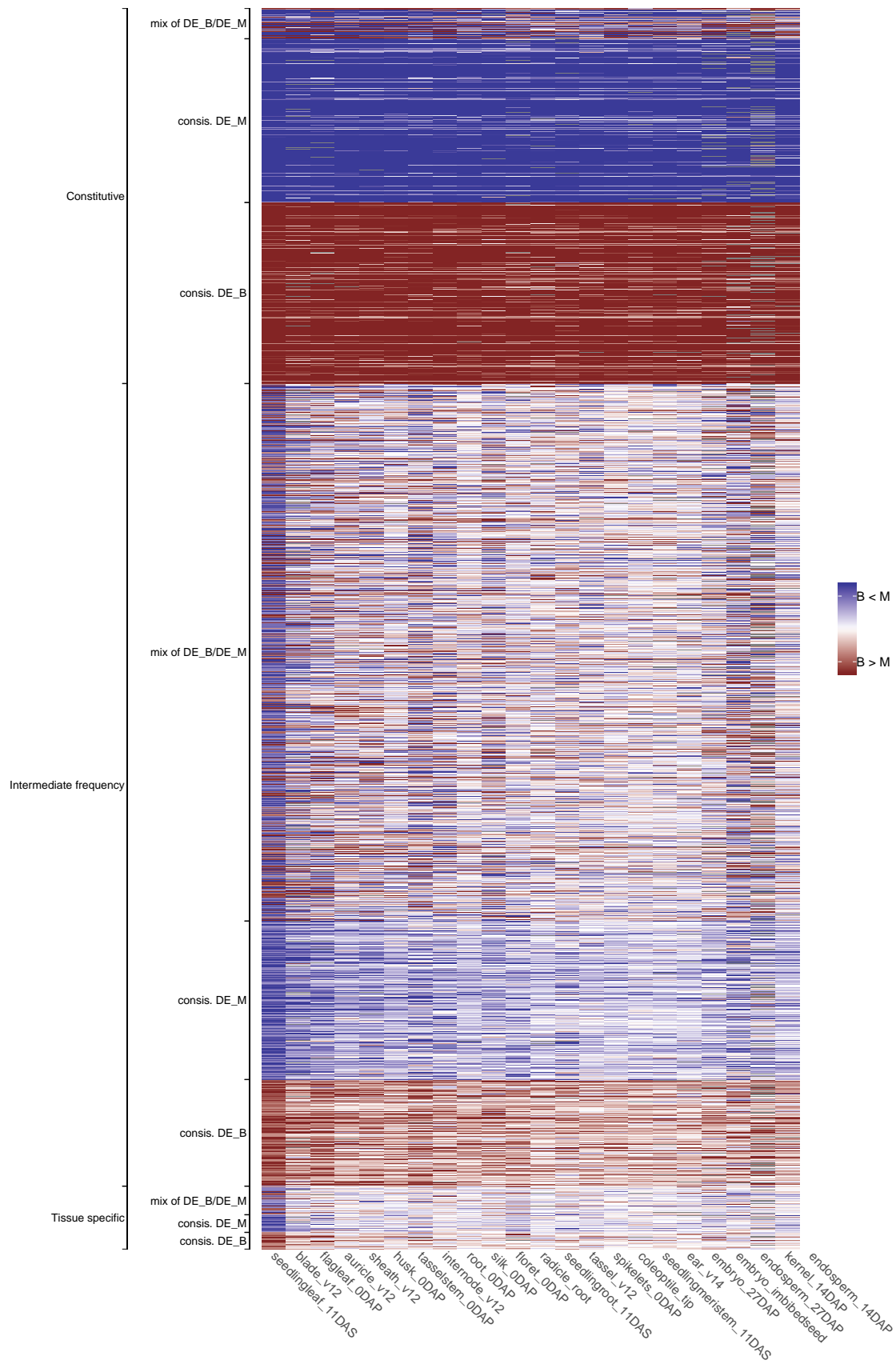


Figure S5. A heatmap is used to visualize expression abundance changes between B73 and Mo17 (i.e.,  $\log_2(\text{Mo17}/\text{B73})$ ) of 3,304 genes that are DE (tissue-wise p-value  $<0.01$  and  $\geq 2$  fold change) in seedling leaf tissue and expressed in at least 20 tissues. Blue color indicates higher expression in Mo17 while red indicates higher B73 expression and white indicates no change in expression in B73 relative to Mo17. Gray color indicates missing values where the gene is silent in both B73 and Mo17 in the corresponding tissue. The genes were first separated into groups based on whether they exhibit tissue-specific, intermediate frequency or constitutive differential expression (as in Figure 2D) and were then separately clustered. Within each of these three groups there are genes that exhibit consistently higher expression of B73 (DE\_B) or Mo17 (DE\_M) as well as some genes that show a mixture of DE\_B and DE\_M.

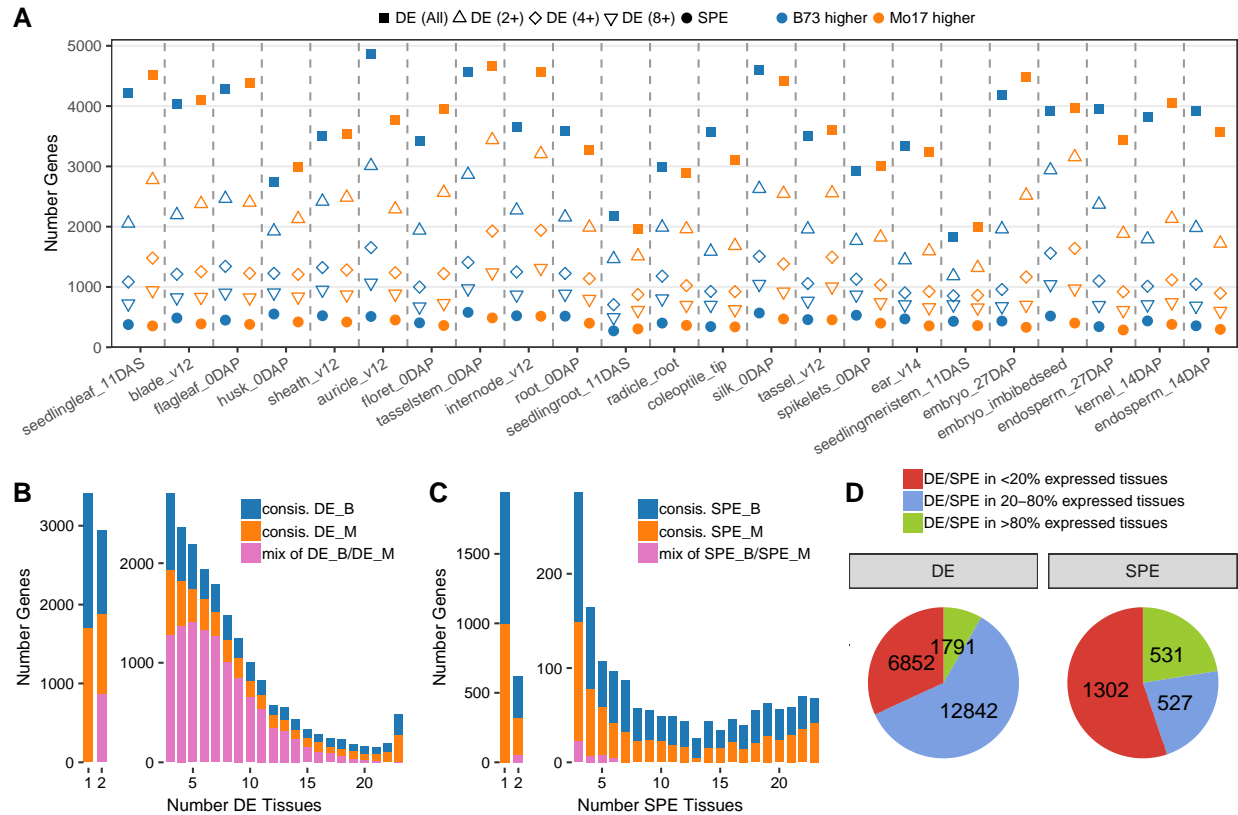


Figure S6. Differential expression analysis based on alignments to the Mo17 reference genome. (A) The number of DEGs for each tissue is indicated by the square symbols with the genotype exhibit higher expression indicated by color (blue - B73 and orange - Mo17). The number of genes with single parent expression (SPE - DEGs with expression <0.1 CPM (Counts per Million) in one parent) for each tissue is shown by the circle. (B) The number of DEGs that are detected in 1-23 tissues is shown. The color indicates which genotypes is more highly expressed as in (A) with pink indicating genes for which some tissues exhibit higher expression for B73 and other tissues with higher expressed for Mo17. (C) The numbers of SPE genes that are detected in 1-23 tissues.

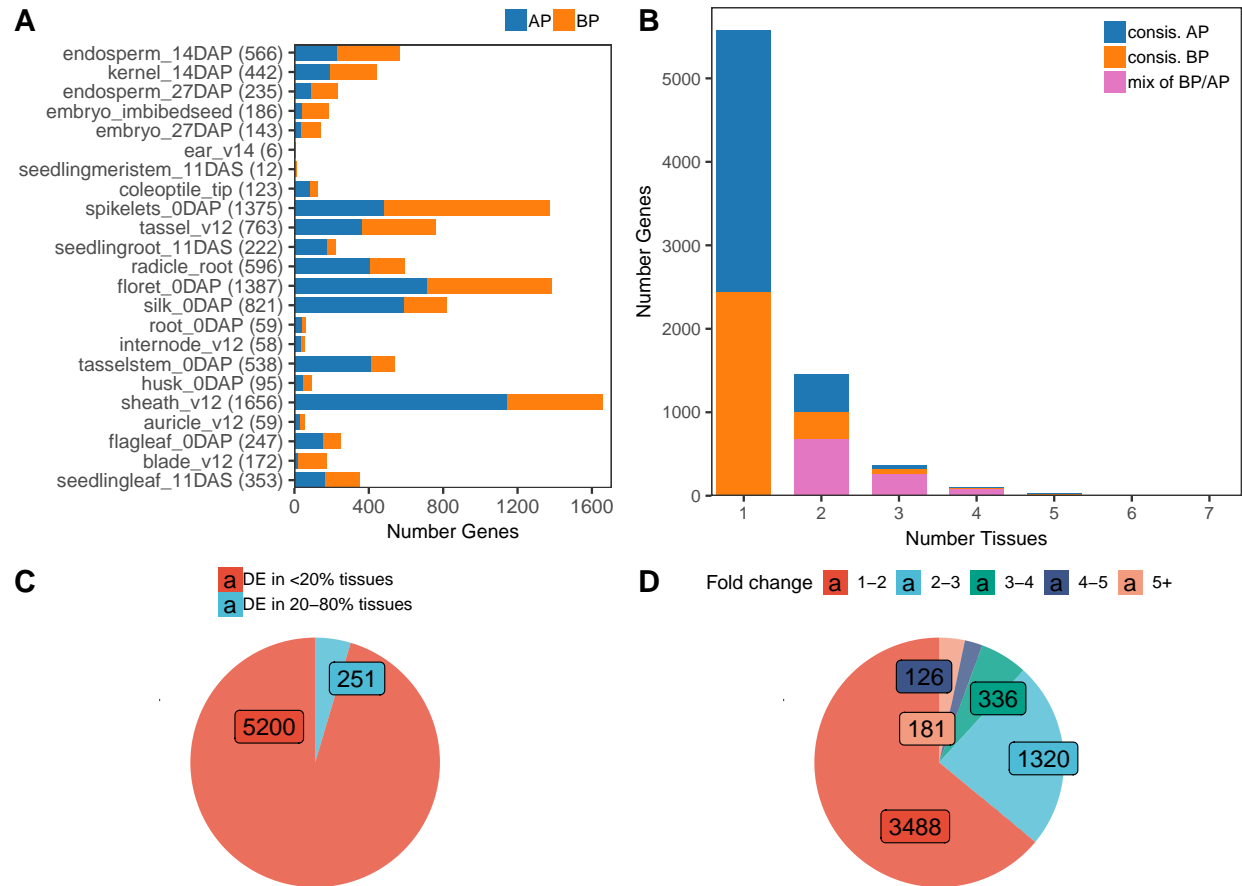


Figure S7. Analysis of non-additive expression for genes that are non-DE in B73 and Mo17. (A) The number of genes that are non-DE between the parents but show above parent (AP, blue) or below parent (BP, orange) expression levels in the hybrid is shown for each tissue. The number in brackets indicates total number of non-additively expressed non-DE genes in each tissue. Some tissues showed extremely low levels of parent-hybrid DE (ear, seedling meristem, root, auricle, coleoptile tip, internode) while other tissues have many more non-additive expression examples between hybrid and parents (sheath, tassel, spikelets, floret, silk). (B) The number of tissues with non-additive expression for these non-DE genes is shown. The color indicates which genotype (parents or hybrid) is more highly expressed (blue - hybrid is higher, orange - parents higher and pink - hybrid is higher than parents in some tissues but lower in others). For the 1,944 genes that exhibit non-additive expression in 2 or more tissues there were 25.6% (498) with consistently above-parent expression in the hybrids and 20.3% (394) with consistent below-parent expression in the hybrids. The remaining 54.1% (1,052) exhibit a mixture of effects with some tissues showing higher hybrid expression and other tissues showing lower hybrid expression. (C) The genes that are expressed in at least 10 tissues and exhibit parent-hybrid DE in at least one tissue were classified as tissue-specific (DE in less than 20% expressed tissues), intermediate frequency (DE in 20-80% expressed tissues) or constitutive (DE in more than 80% of expressed tissues). There are very few examples of non-additive patterns for these non-DE genes that occur in >20% of expressed tissues and there are no examples with non-additivity in >80% of the tissues. (D) The relative expression changes between parents and hybrid for these non-additive genes was assessed. The majority of these genes were just passing the 2-fold change cut-off used for DE and only 181 (3.3%)

of these genes exhibit at least 5-fold change in expression in the hybrid relative to the parents.

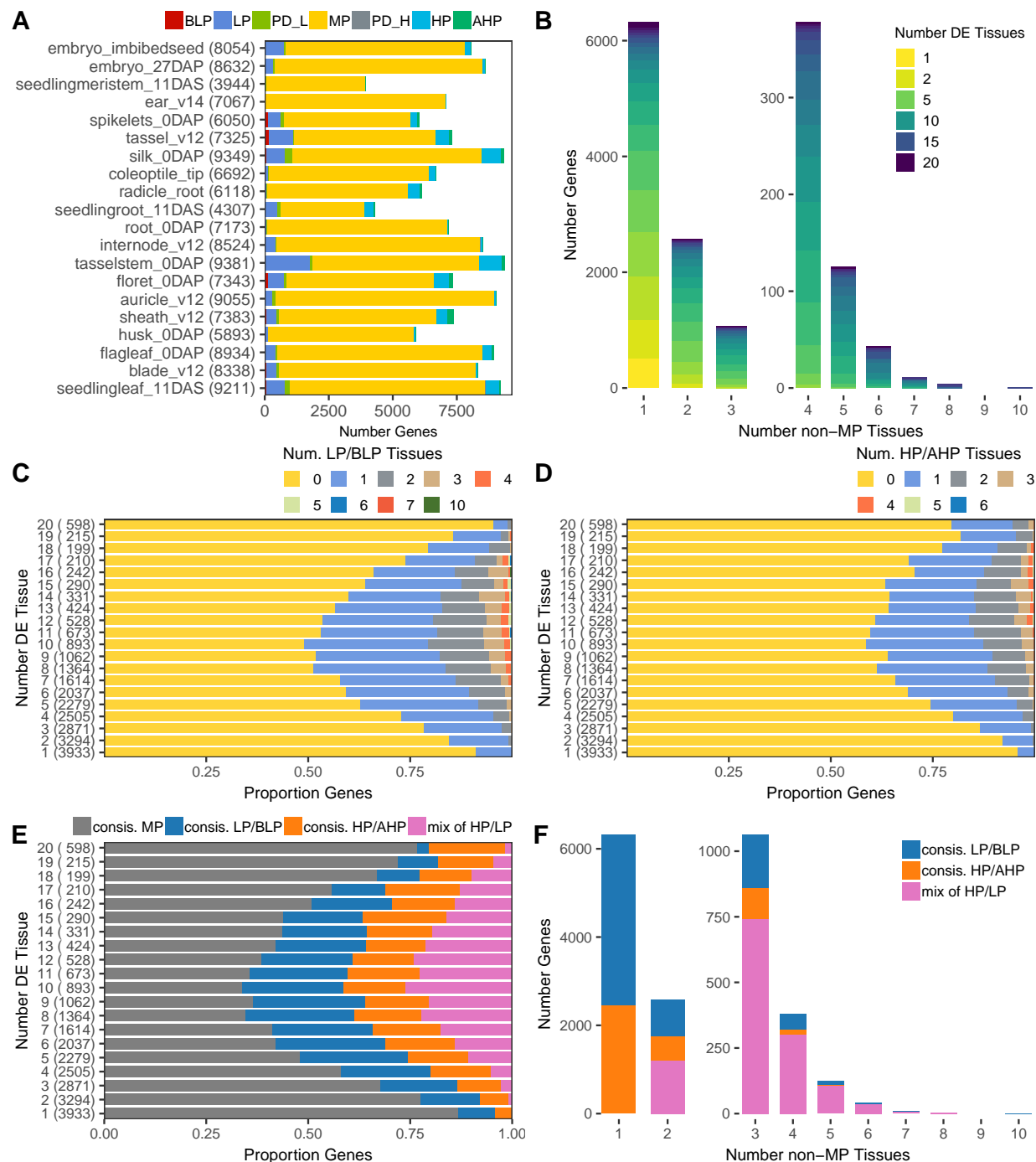


Figure S8. Analysis of additivity patterns for genes that are DE between parents across tissues. (A) The number of genes assigned to each additive or non-additive inheritance pattern in each tissue. MP: mid-parent like; LP: low-parent like; BLP: below low-parent; HP: high-parent like; AHP: above high-parent; PD\_H: partial dominance higher than mid-parent; PD\_L: partial dominance lower than mid-parent. (B) Genes were classified according to the number of tissues with non-MP expression patterns (x-axis). Within each category a heatmap is used to visualize the number of tissues with differential expression between parents in 1-20 tissues. (C-D) Bar plot shows among all genes that are DE in 1-20 tissues (y-axis) the proportion with LP/BLP (panel C) or HP/AHP

(panel D) pattern shared across different number of tissues (1-10). (E) Bar plot shows among all genes that are DE in 1-20 tissues (y-axis), the proportion that are classified as “consistent MP”, “consistent LP/BLP”, “consistent HP/AHP” or “mix of HP/LP” based on whether the observed non-additive pattern switches direction among tissues. For panels C through E numbers in brackets are the total number of genes in each bar category (i.e., number of genes DE in 1-20 tissues). (F) Analogous to panel E but rather than proportion, the number of genes showing non-MP patterns in 1-10 tissues were shown, with color coding the same as panel E.



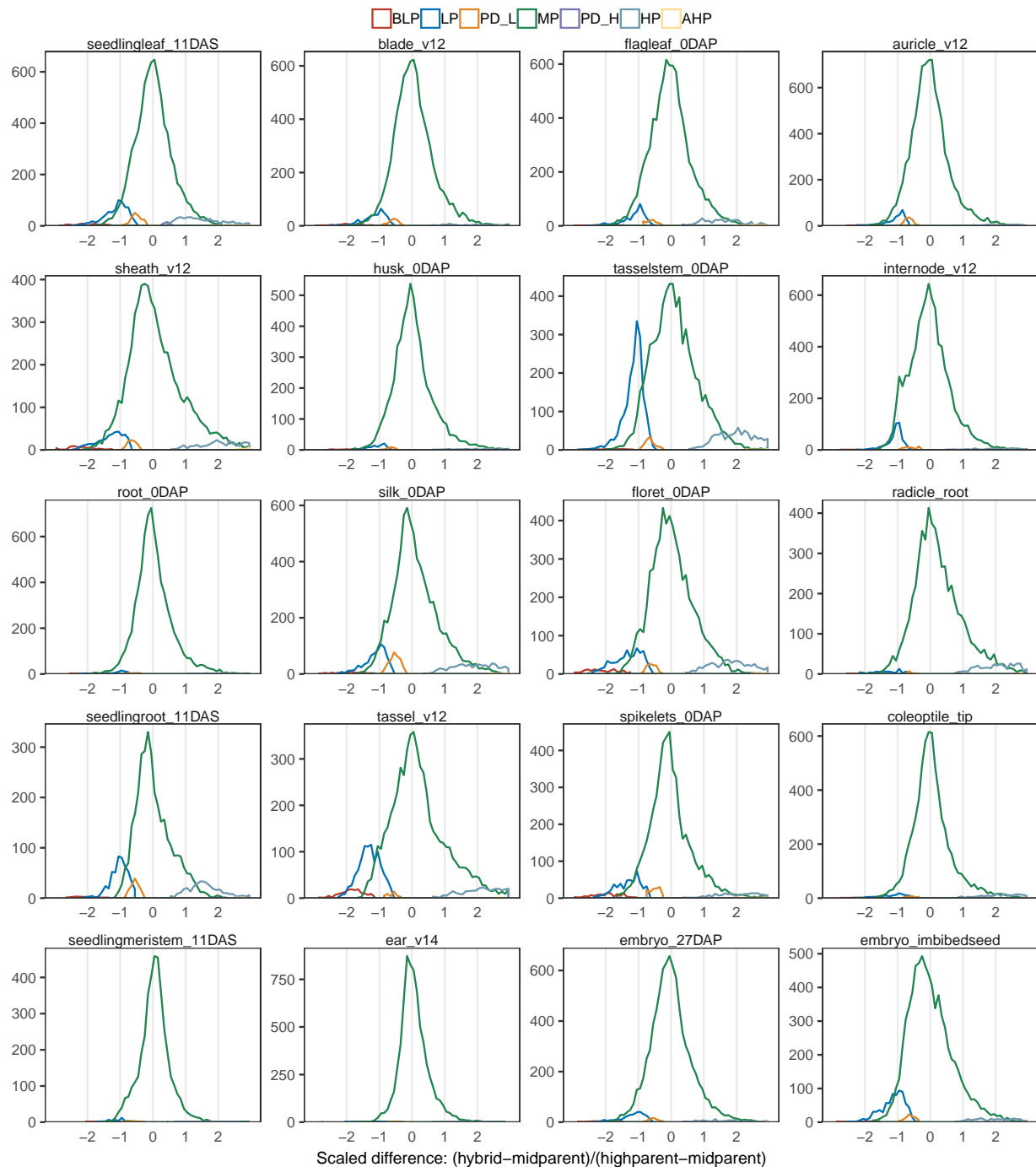


Figure S9. Frequency distribution of scaled difference values (between hybrid and mid-parent, i.e., D/A values) for genes that are assigned to different inheritance patterns.

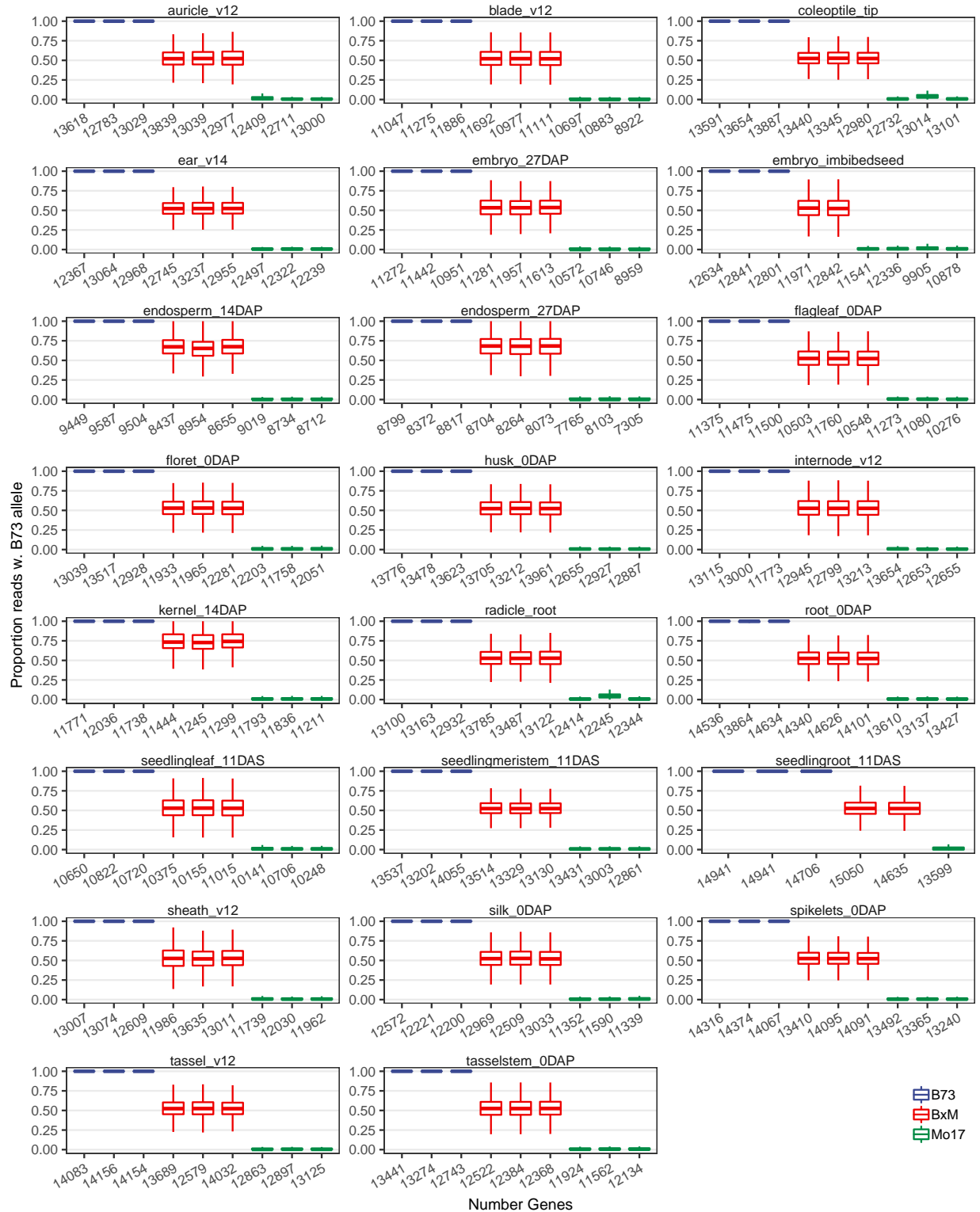


Figure S10. Analysis of allele-specific expression. For each sample we counted the number of reads carrying the Mo17 allele (SNP) or the B73 allele for each gene. Numbers below x-axis show the number of genes with at least 10 allele-specific reads, while y-axis gives the distribution of the B73 allele proportions for all genes in each sample. Not surprisingly, transcripts in inbred samples

all carry the corresponding B73 or Mo17 allele, while genes in hybrid samples have varying levels of allele proportion but center around 50% (for endosperm, the expectation becomes 67% due to the 2:1 parental ratio).

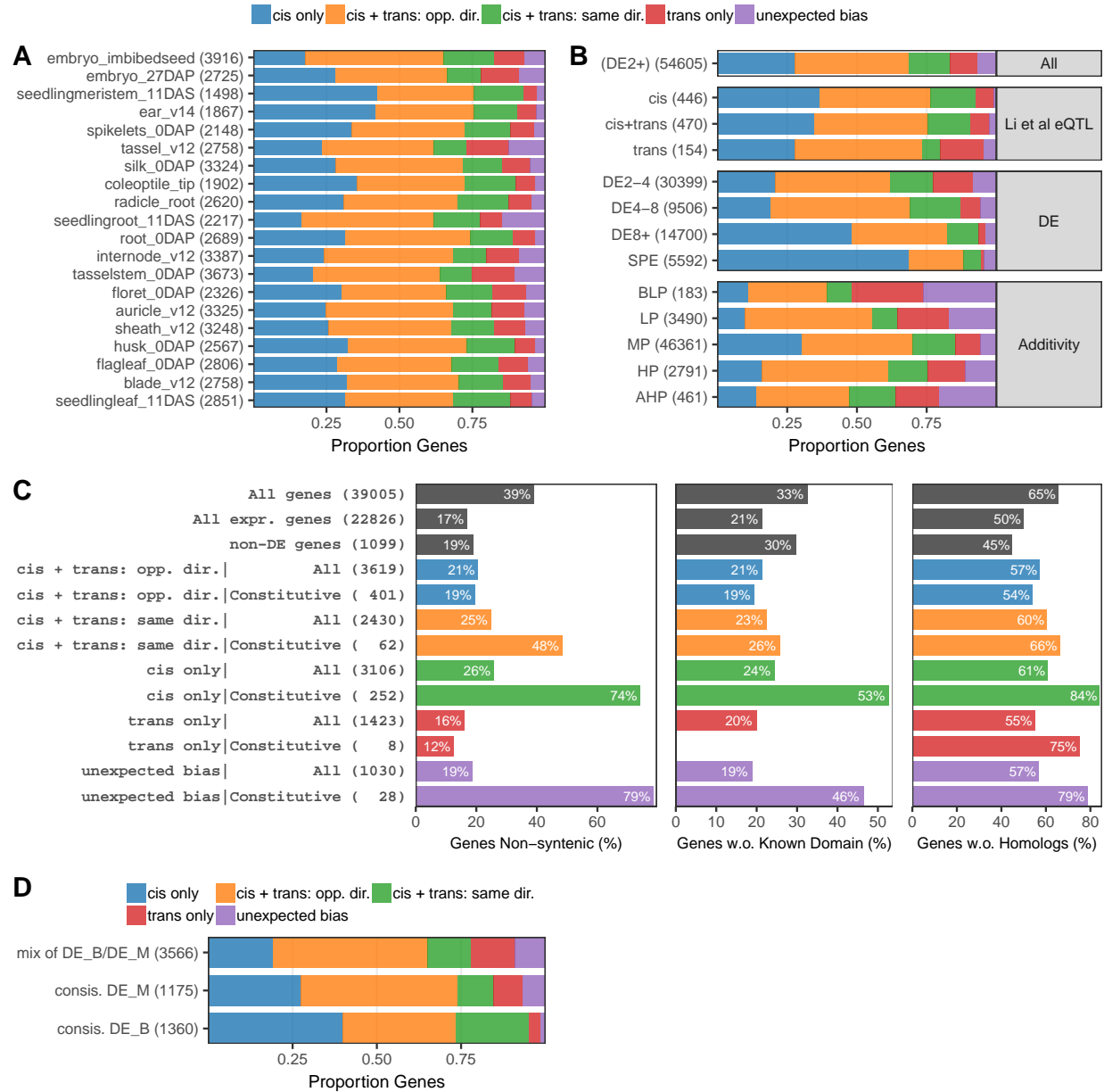


Figure S11. Analysis of regulatory variation across tissues and developmental stages. (A) The proportion of genes classified into each pattern of regulatory variation is shown for each tissue (cis-only, trans-only, cis+trans: opposite direction, cis+trans: same direction and unexpected) in each tissue. The numbers in parentheses reflect the number of genes classified in each tissue. (B) A non-redundant list of gene/tissue combinations of regulatory classifications was assessed. In total there are 54,605 gene/tissue combinations with a classification for regulatory variation (DE2+). The distribution of classifications for genes characterized by previous eQTL mapping study as cis- or trans- regulated, with varying levels of differential expression, SPE or additivity patterns were assessed. (C) The proportion of genes under different regulatory patterns that are non-syntenic, lack any known domains (Interproscan) or lack any homologs (arabidopsis of uniprot.plants) was determined and compared to all genes, all expressed genes (i.e., genes expressed in at least one out of the total 23 tissues) and non-DE genes (genes not showing DE in any of the 23 tissues). (D) The percentage of different regulatory patterns for the set of genes that have consistent B73

higher expression (consis. DE\_B), consistent Mo17 higher expression (consis. DE\_M) or a mix of B73 higher expression and Mo17 higher expression across tissues was shown.

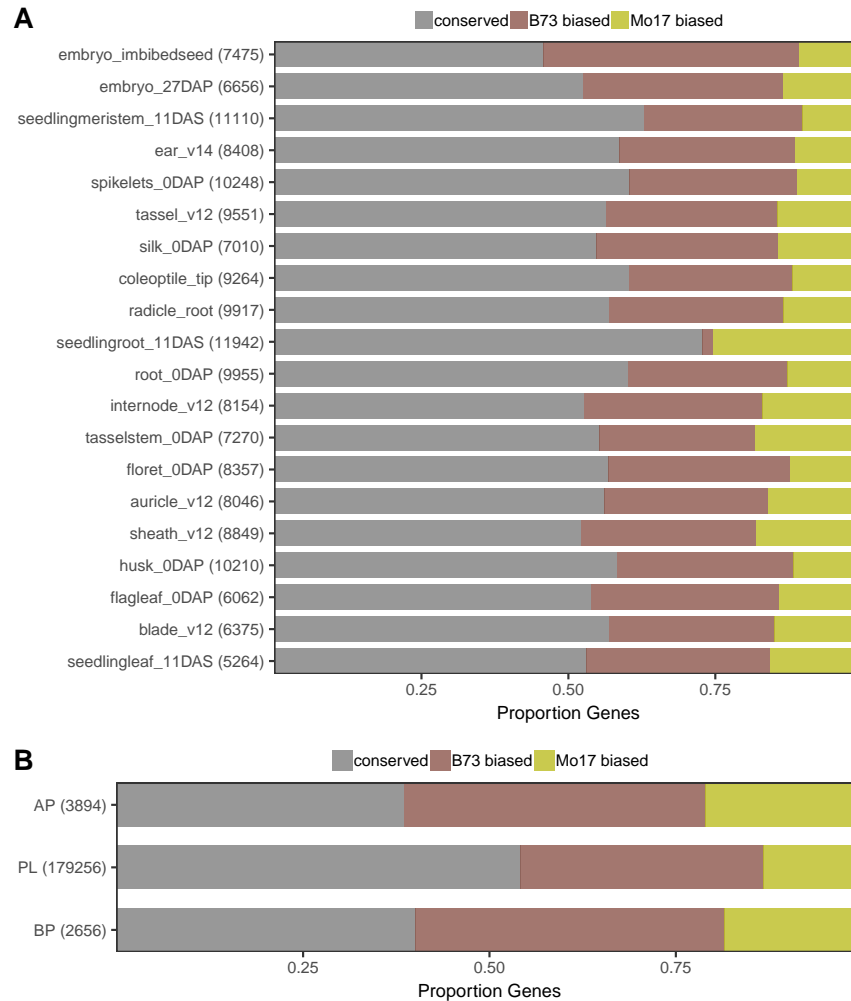


Figure S12. Analysis of allelic bias of non-DE genes across tissues. (A) Proportion of genes showing B73-biased or Mo17-biased allelic expression in each tissue. (B) DE genes between parents and hybrid are enriched in biased allelic expression in the hybrid. Bar shows across all tissues the proportion of DE genes (AP - hybrid is above parents or BP - hybrid is below parents) or non-DE genes with conserved allelic ratio, B73-biased allelic ratio or Mo17-biased allelic ratio.

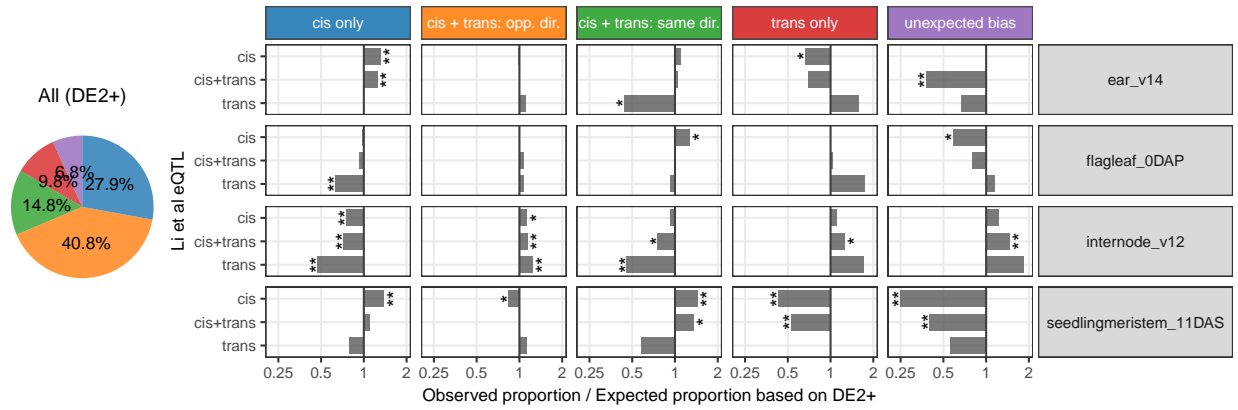


Figure S13. Comparison of regulatory classification approaches based on eQTL mapping and ASE analysis. The pie-chart (left) shows the proportion of all differentially expressed genes (between the two parents) that were assigned to different regulatory mechanisms across all tissues. The plots on the right show the enrichment or depletion (as fold change relative to background proportion from the left pie-chart) for genes that were characterized by previous eQTL study (in Shoot Apex Meristem) to be regulated by only cis-eQTL(s), only trans-eQTL(s) or by both cis-eQTL(s) and trans-eQTL(s). The comparison was made using the ASE data from seedling meristem tissue (closest to SAM used in the eQTL analysis) as well as three other tissues (flag leaf, root and ear). For each comparison the proportion of each regulatory classification was compared to background proportion (left pie-chart) with the ratio plotted as bars along x-axis. P-values for each comparison were determined using hypergeometric test (lower.tail = FALSE for enrichment and lower.tail = TRUE for depletion) and labelled as "\*" (P < 0.01) or "\*\*\*" (P < 0.001).